NASA/CR–2011-216884

Open Circuit Resonant Sensors for Composite Damage Detection and Diagnosis

John J. Mielnik, Jr.
Lockheed Martin Corporation, Hampton, Virginia

January 2011

NASA STI Program . . . in Profile

Since its founding, NASA has been dedicated to the advancement of aeronautics and space science. The NASA scientific and technical information (STI) program plays a key part in helping NASA maintain this important role.

The NASA STI program operates under the auspices of the Agency Chief Information Officer. It collects, organizes, provides for archiving, and disseminates NASA's STI. The NASA STI program provides access to the NASA Aeronautics and Space Database and its public interface, the NASA Technical Report Server, thus providing one of the largest collections of aeronautical and space science STI in the world. Results are published in both non-NASA channels and by NASA in the NASA STI Report Series, which includes the following report types:

- TECHNICAL PUBLICATION. Reports of completed research or a major significant phase of research that present the results of NASA programs and include extensive data or theoretical analysis. Includes compilations of significant scientific and technical data and information deemed to be of continuing reference value. NASA counterpart of peer-reviewed formal professional papers, but having less stringent limitations on manuscript length and extent of graphic presentations.

- TECHNICAL MEMORANDUM. Scientific and technical findings that are preliminary or of specialized interest, e.g., quick release reports, working papers, and bibliographies that contain minimal annotation. Does not contain extensive analysis.

- CONTRACTOR REPORT. Scientific and technical findings by NASA-sponsored contractors and grantees.

- CONFERENCE PUBLICATION. Collected papers from scientific and technical conferences, symposia, seminars, or other meetings sponsored or co-sponsored by NASA.

- SPECIAL PUBLICATION. Scientific, technical, or historical information from NASA programs, projects, and missions, often concerned with subjects having substantial public interest.

- TECHNICAL TRANSLATION. English-language translations of foreign scientific and technical material pertinent to NASA's mission.

Specialized services also include creating custom thesauri, building customized databases, and organizing and publishing research results.

For more information about the NASA STI program, see the following:

- Access the NASA STI program home page at *http://www.sti.nasa.gov*

- E-mail your question via the Internet to help@sti.nasa.gov

- Fax your question to the NASA STI Help Desk at 443-757-5803

- Phone the NASA STI Help Desk at 443-757-5802

- Write to:
  NASA STI Help Desk
  NASA Center for AeroSpace Information
  7115 Standard Drive
  Hanover, MD 21076-1320

Open Circuit Resonant Sensors for Composite Damage Detection and Diagnosis

John J. Mielnik, Jr.
Lockheed Martin Corporation, Hampton, Virginia

PREFACE

This document constitutes the final report of the Integrated Vehicle Health Management (IVHM) task order entailing Open Circuit Resonant Sensors for Composite Diagnosis.

The Task order number was 087D3-NNL10AM09T. This research and development effort was funded using the American Recovery and Reinvestment Act (ARRA) funding with direct guidance from the NASA Technical Monitor. The final completion of the report was accomplished under Task Order number NNL10AM25T.

The NASA Technical Monitor for this task is Sandra V. Koppen.

The work was accomplished by engineering support personnel of the Lockheed Martin Corporation.

Table of Contents

LIST OF FIGURES

LIST OF ACRONYNS

Acronym	Meaning
IVHM	Integrated Vehicle Health Management
ESB	Electromagnetics & Sensors Branch
HIRF	High Intensity Radiated Fields
NASA	National Aeronautics and Space Administration
LaRC	Langley Research Center
RF	Radio Frequency
UV	Ultra Violet
NDT	Non Destructive Test
EM	Electro Magnetic
BW	Bandwidth
D.C.	Direct Current
CAD	Computer Aided Design
KNK	Klik-N-Kut
PNA	Performance Network Analyzer

LIST OF SYMBOLS

Symbol	Meaning
L	Inductance
C	Capacitance
R	Resistance
f	Frequency
π	PI
Q	Quality Factor
BW	Bandwidth
N	Number of turns (of spiral)
μ_0	Permeability of free space ($4\pi \times 10^{-7}$)
μ_r	Relative permeability of medium
a	Wire radius

1.0 SUMMARY

Under the Integrated Vehicle Health Management (IVHM) program work was begun to investigate the feasibility of sensor systems for detecting and diagnosing damage to aircraft composite structures and materials. Specific interest for this study was in damage initiated by environmental storm hazards and the direct effect of lightning strikes on the material structures of a composite aircraft in flight. The research and development for this work was sponsored by the Electromagnetics and Sensors Branch (ESB) and conducted in the High Intensity Radiated Fields (HIRF) Laboratory of the NASA Langley Research Center (LaRC).

An internal partnership for design guidance was formed with Dr. Stanley Woodard of NASA's Research Directorate. Dr. Woodard is the inventor of SansEC^{tm} resonant sensor technology which was leveraged and expanded in notion to develop a proof-of-concept composite damage detection and diagnosis sensor. In determining the feasibility of using open circuit resonant sensors for composite aircraft damage detection and diagnosis an extensive literature search and review of published works pertaining to lightning, composite materials, and open circuit resonant sensor designs and applications was performed.

Damage in composite materials is theorized to be associated with a change in the electrical impedance in the vicinity of the damaged area. Passive open circuit resonant sensors can be used to remotely detect such an impedance change by measuring the resonance response of the sensor. The associated resonance response is quantifiable in frequency, amplitude, bandwidth, and phase and can be correlated to the level of damage inflicted on a composite material. Open circuit resonant sensors provide an added advantage in that they will continue to function should the sensor itself become damaged. By additional means of geometry and design, the electrically quantifiable information associated with the sensor response can be used for composite material lightning damage detection and diagnosis.

A series of open circuit resonant sensors was designed, fabricated, characterized, and determined to be a potentially viable means for damage detection and diagnosis of composite materials. Further development of the sensor is needed to provide multifunctional roles which include functioning as lightning protection and radio frequency (RF) shielding. The results of this research and development effort are documented in this report.

2.0 INTRODUCTION

Composite materials have been in use for several thousands of years and developments in material science over the past several decades have resulted in an increased use. Composite materials provide the ability to design and produce lighter and stronger structures. In addition to the strength to weight ratio, the advantage of being able to be formed into complex shapes has made composites a desirable material in many industries. Figure 1(a-f) illustrates a small example of the broad spectrum of composite material uses from automobiles to satellites.
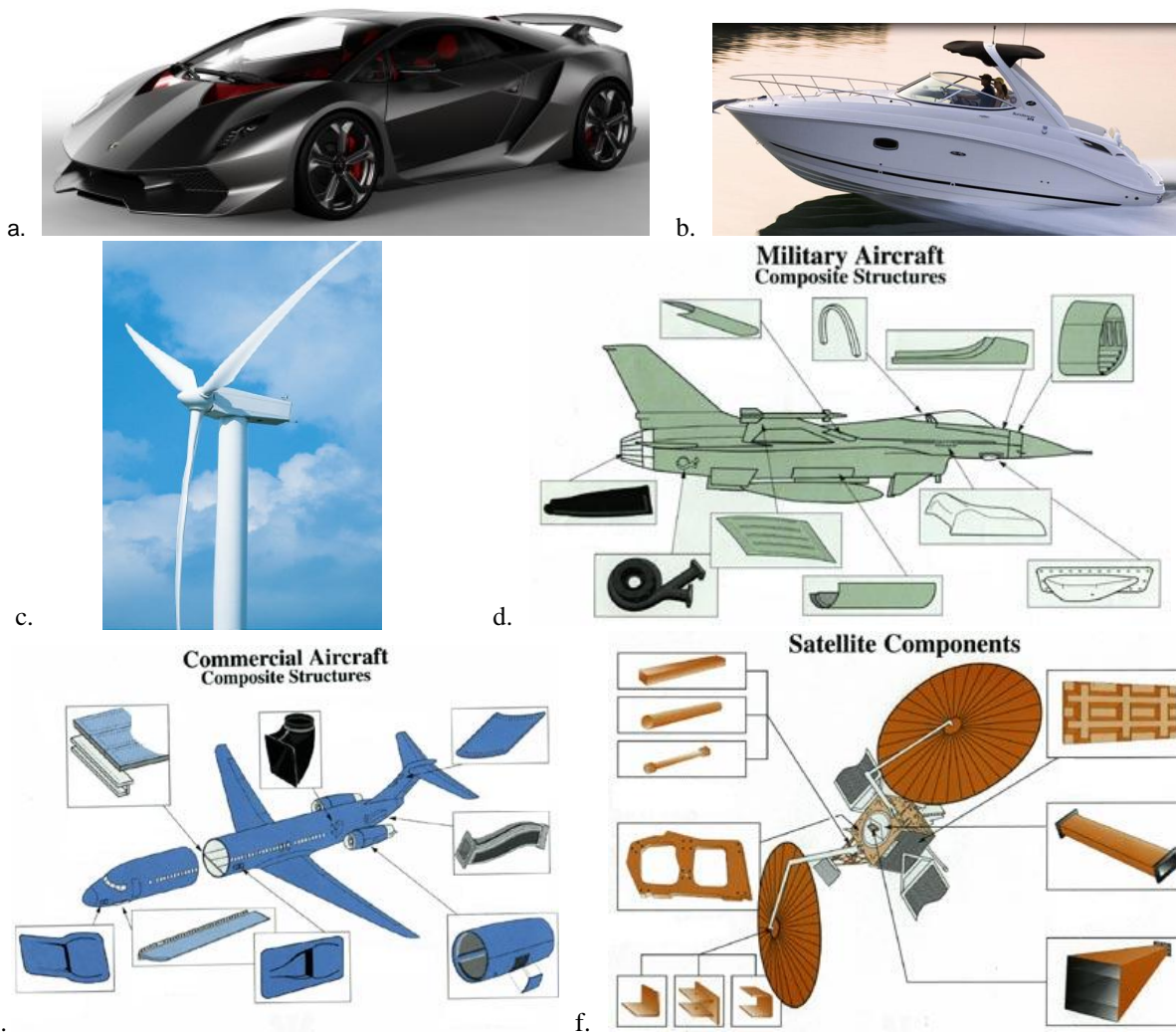
Figure 1. Examples of composite material use. a. Lamborghini Sesto Elemento makes extensive use of composites for interior and exterior components [1]; b.Sea Ray 280 composite hull [2]; c. Composite wind turbine blades [3]; d. Composite components on F-16 [4] ; e. Composite components on commercial aircraft [5]; f. Composite components on satellite [6].

Aviation has seen an increase in the use of composite materials. Modern air vehicles increasingly use composite materials for high strength and stiffness with minimal weight. Today's aircraft incorporate substantial amounts of carbon, aramid, or fiberglass composite materials. Airframe manufacturers have gone from using composite panels for cosmetic coverings and fairings to empennage, wing, fuselage structures, and turbine blades.

The increased usage also means an increased potential for damage to and/or failure of the composite materials. While we currently understand and can predict failure modes of composite structures with a high degree of accuracy, it is difficult to predict the degree of composite damage or incipient states of failure while in use. A means of detection and diagnosis in real time would be a highly desirable resource in enhancing safety.

The purpose of this report is to document the proof-of-concept exploration in the use of open circuit resonant sensors for damage detection and diagnosis of composite materials. This is ultimately focused toward future use onboard aircraft, but this is not to be considered a limiting restraint as composites have found use in many industries where damage detection and diagnosis would be a viable asset as well. Ideally, this sensor would ultimately serve a multifunctional role providing damage detection and diagnosis, lightning protection, and RF shielding.

2.1 Background

Composite materials, often referred to as composites, are a combination comprised of two or more materials which are combined on a macroscopic level. The constituent materials retain their individual identities and do not merge or blend together [7]. Typically, composites are composed of a reinforcement which is embedded in a matrix or resin. The reinforcement materials often are fibers, particles, flakes, etc. Figure 2 is an example of a carbon fiber weave which is commonly used as a reinforcing material.
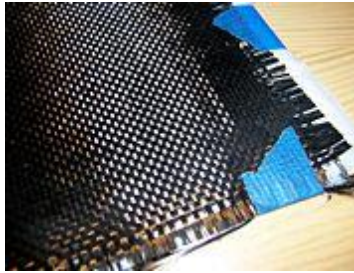
Figure 2. Carbon fiber weave.

Polymers, metals, ceramics, etc. act as the matrix and hold the reinforcement material to the desired shape. The reinforcement material enhances the mechanical properties of the resin. The combination yields a material exhibiting increased strength when compared to the individual components. Concrete and plywood are two well known and commonly used composite materials. Composite materials formed from reinforcements of fiberglass or carbon (graphite) are becoming widely used in many industries and generally have a higher strength to weight ratio compared to metallic structures of comparable dimension. Along with strength and weight savings, other factors exhibited which make composites attractive to the aviation industry are resistance to fatigue, corrosion, and the ability to be formed into complex shapes [8].

Similar to metallic alloys designed for specific characteristics in metal, composite hybrid materials are created with the addition of complimentary materials. The addition of materials to the basic carbon fiber/epoxy matrix aids in obtaining materials with specific properties, such as increased fracture or impact resistance. Kevlar and boron fibers are commonly used.

Composites are typically comprised of several layers or plies of the reinforcement material. The orientation of the plies is a factor in the strength of the material along its various axes. A typical orientation involves the plies at 90° to each other and is referred to as 0°-90°. Figure 3 illustrates the layup of a multi-ply laminated composite panel with the individual lamina oriented 90° to the subsequent layer.
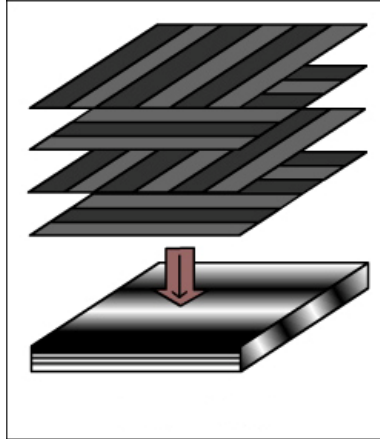
Figure 3. Example of a multi-ply composite laminate composed of individual lamina showing orientation of plies at right angles to each other [9].

Like most materials, composites are subject to damage and degradation. Damage may be inflicted physically or environmentally. Flaws in production can also cause a decrease in a composite component's integrity. Stress from compression, tension, shear, and torsion are among the possible forces acting on a composite structure that can cause damage or lead to failure. Environmental factors, such as moisture, lightning, and ultra violet (UV) radiation can result in a degradation of the material over time.

Obvious damage can be detected visually and is readily apparent and requires little equipment. Determining the extent of the damage requires the use of specialized test equipment and methods. As seen in figure 4, the initial damage is obvious [10]. The extent of transferred stress or the amount of hidden damage is not. Surrounding areas can be placed under loads and weakened without exhibiting any indications on the outer surface.

a.   b.   c.

Figure 4. Examples of obvious damage. a. Damage to radome caused by hail; b. Bird strike to horizontal stabilizer; c. Jacking incident during maintenance.

Damage that is hidden or not obvious presents a challenge when it comes to the initial detecting and/or determining the extent of the damage to the structural integrity of the affected component(s). Composite panels can exhibit only minor damage on the exterior surface, but internal damage may exist which can cause a loss in structural integrity. Figures 5 and 6 illustrate instances of internal and hidden damage.

Figure 5 is a side view showing delaminated plies and internal buckling, but the top surface is relatively free from visual damage indication. The damage was caused by an impact to the upper surface [10].
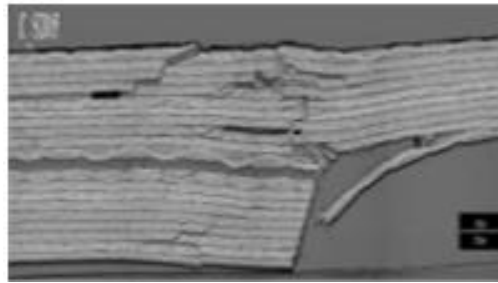
Figure 5. Delaminated plies and buckling.

Figure 6 depicts examples of defects discovered using various non-destructive test (NDT) methods. The examples in figure 6 show defects that most likely occurred during manufacturing (voids, porosity) and during use (chemical attack, oxidation cracks, micro-cracking, and buckling) [11].
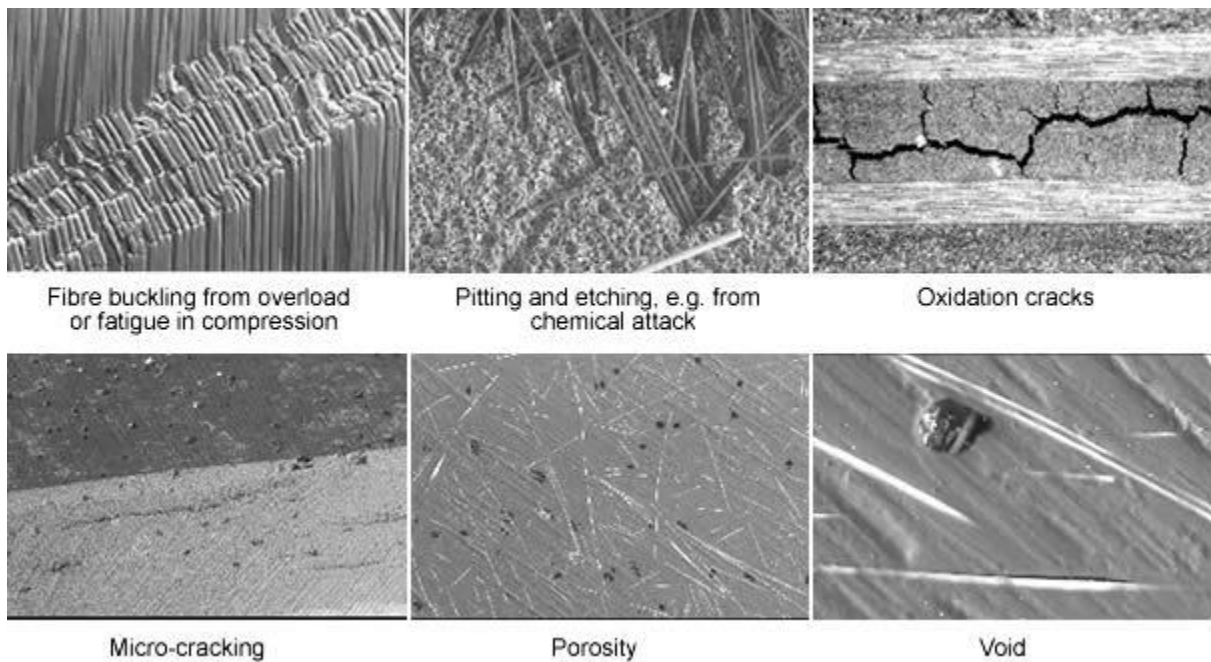
Figure 6. Examples of hidden defects and damage.

2.2   Problem

Not all composite damage requires an immediate repair. With any type of construction there is a built in safety margin. The trouble lies in detecting and diagnosing damage in real time and during use to determine the criticality. The current methods for inspecting and determining the degree of damage that exists to the composite material are performed when the component is not in use. For aircraft, this is on the ground after a flight or during an inspection. Once on the ground, the continued risk to human safety is typically minimal. The ability to detect and diagnose the level of damage sustained or the incipient stages of hidden damage would be a significant asset to the fight crew and maintenance personnel adding

an additional level of safety.

Presently, there is no means to accurately detect and diagnose the extent of damage a composite structure has sustained and/or indicate the beginning stages of a potential catastrophic failure in real-time. Unless pilots have a reason to believe there is a problem they continue to fly. As with other industries, if there is no indication of an unsafe condition then operation will continue. Outside surfaces cannot be seen entirely during flight. Damage may appear minor on the outside, but the panel may have delaminated plies or other damage to the inside. Due to the lightning current path or load stress transfer, damage may be in an area away from the initial damage. Damage to surrounding areas could be overlooked or missed based on a visual inspection. The component or structure could fail prior to being detected. There is no way to determine the level of damage in-flight. This in turn could lead to additional damage to surrounding property, structures, and/or loss of life. Detection of the damage or degraded state of the composite structure in real-time is the focus of this research.

2.3 Objective

Creating a means to detect and assist in diagnosing damage to composites would allow for informed decisions by the user regarding safe continued operations. Open circuit resonant sensors lend themselves to filling this need. This task was focused on providing a proof of concept design utilizing an open circuit resonant sensor and demonstrating the ability to detect damage to a composite panel. The data gathered can be used for subsequent design iterations to further advance the conceptual use of open circuit resonant sensors on composites. Further advances may result in a sensor with multifunctional roles providing damage detection and diagnosis, lightning protection, and RF shielding.

2.4 Scope

Composite materials have applications beyond aircraft use as presented earlier. The applications of this sensor are focused on damage detection and diagnosis of composite materials in use on aircraft with the ability to serve a multifunctional role that includes lightning protection and RF shielding. This concept may be adaptable to other industries and applications.

2.5 Approach

The approach taken led to a methodical design, development, and test of an open circuit resonant sensor for detecting composite panel damage. The steps included a literature search to investigate work pertaining to composite materials and open circuit resonant design and applications, the design of a sensor based on the literature search, development and fabrication of a sensor based on the initial design, development of a test plan, test according to the plan, and documentation of the results.

Modeling of the open circuit resonant sensor design was also accomplished as a parallel effort using FEKO. FEKO is an electromagnetic (EM) analysis software suite. Use of the FEKO software was done to provide additional data for comparison with the actual measured results. This will also allow for a level of confidence for future modeling of the sensors to alleviate the need to fabricate sensors and perform testing on each sensor design. Instead, this will allow resources to be applied to the sensor designs that predict the intended design characteristics and reduce the need for trial and error setups.

The use of composite materials is ever increasing and the composition of the panel is largely determined

by the intended area of use. A multitude of choices exist and it was determined that a standard ¼" thick structural fiberglass composite panel would be used. Much of this was based on the availability and cost of the material. The panels were fourteen inches square.

Figure 7. ¼ inch thick structural fiberglass panel.

Damage to the composite panel was limited to a simulated crack and a series of 5/16 inch holes drilled simulating a puncture. These types of simulated damage were selected because of the ability to be easily recreated for repeatability if needed. Figure 8 illustrates the fiberglass panel with the crack and punctures.
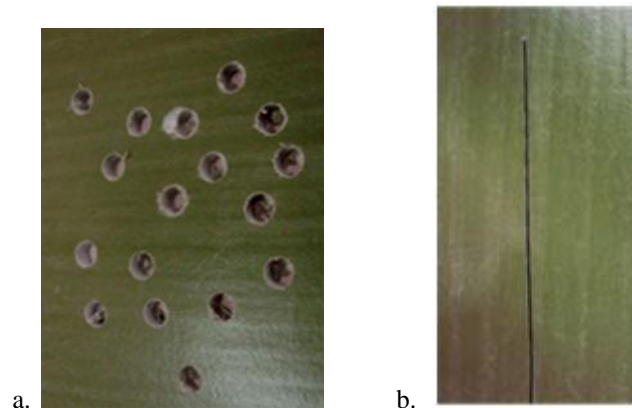
a.   b.
Figure 8. Simulated damage to fiberglass panels. (a) holes (puncture), (b) crack.

3.0   LITERATURE REVIEW

A literature search was performed in order to investigate work pertaining to composite materials, spiral inductors, and open circuit resonant design and applications. The information gathered from the literature search provided an adequate amount of information to design a series of open circuit resonant sensors and establish baseline data to initiate conceptual testing for damage detection.

4.0   SENSOR DESIGN

4.1   Sensor Background

The SansEC^{TM} is an open circuit resonant sensor technology developed by Dr. Stanley Woodard and his colleagues at NASA Langley Research Center. The HIRF Lab at LaRC is leveraging this technology with plans to develop it into an aircraft composite material damage detection and diagnosis system through focused research and development. The name SansEC^{TM} implies the open circuit approach through the translation Sans (without) EC (Electrical Connection). The sensor provides all the functionality of a traditional closed resonant circuit having, by geometrical design, an inductor element, a capacitor element, and a resistor element, but it does so without requiring any direct electrical connections to a generating source. The sensor is passive, but it is energized by an electromagnetic field generated remotely from the sensor and produces magnetic field responses when electrically stimulated. For simplicity, the term SansEC^{TM} sensor and open circuit resonant sensors will be used interchangeably and referenced as resonant sensors from here on out unless a distinction is necessary.

The sensor baseline design is a single physical component of geometric design constructed of conductive material. There is no single point on the circuit that if damaged destroys the functionality of the circuit. The resonant sensor is essentially an electrical inductor in the form of a planar spiral. Figure 9 illustrates a square spiral resonant sensor. The sensor does not utilize a distinct built in capacitor or resistor, but rather the inherent capacitance and resistance of the geometric design. The inductance (L) is the sum of all the self and mutual inductances of the individual trace interactions. The capacitance (C) is an inherent result of the width between the spiral traces and substrate dielectric and the resistance (R) is largely dependent upon the overall trace dimensions. Figure 10 is the schematic representation. If the sensor itself is damaged, such as torn or punctured, it still functions but with a different frequency response. Depending on the failure and its location, a single sensor or multiple coupled sensors will now exist and still maintain function [12]. This robustness of functionality makes these types of sensors highly effective in detecting and diagnosing damage.

Figure 9. Square spiral sensor.
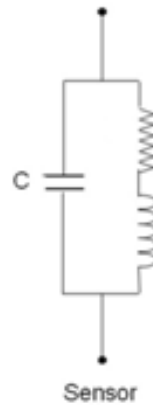
Figure 10. Schematic representation of sensor.

Placing the sensor upon a non-conductive substrate material, such as a composite panel, alters the

13

sensor's free space characteristics of frequency, amplitude, and bandwidth. The substrate material on which the sensor is placed or attached acts as a dielectric. Any changes of this modified baseline characteristic can be used to detect changes physically to the sensor or the substrate upon which it is placed or embedded. Comparisons of these changes from the baseline frequency, amplitude, or bandwidth response produce unique signatures that can be correlated to the detection of damage.

The baseline frequency corresponds to the resonant frequency of the sensor. The resonant frequency is determined by the interaction of the overall inductance and capacitance of the sensor. As seen by equation (1), the equation for resonant frequency of a LC circuit, resonance is inversely proportional to the square root of either L or C [13].

$$f = \frac{1}{2\pi\sqrt{LC}}$$
Eq. (1)

Where f is the frequency in hertz, C is capacitance in farads, and L is inductance in henrys. The resonant frequency increases as the inductance decreases. The same effect is true if capacitance varies with inductance remaining constant.

The resistance of the resonant sensor has the greatest affect on the selectivity or quality factor (Q) of the sensor which in turn affects the bandwidth. The simple definition of Q is the amount of energy stored over the energy loss in one cycle. In terms of inductors, Q becomes the ratio of peak magnetic energy minus peak electric energy. The inductance is also a factor in determining the Q, but resistance exerts a greater influence with inductance playing a greater role on the center frequency. The higher the quality factor the sharper the response curve at the resonant frequency. This sharper response curve in turn results in a smaller bandwidth (BW). The Q of a circuit can be determined by calculation or using measured data. When using measured data, the Q can be found using equation (2) [13].

$$Q = \frac{f}{\Delta f}$$
Eq. (2)

Where Q is the quality factor, f is the resonant frequency, and Δf is the difference in frequency at the 3dB power points. The theoretical calculation of the quality factor takes into account the resistance of the circuit and is determined using equation (3) [13].

$$Q = \frac{2\pi f L}{R}$$
Eq. (3)

Where Q is the quality factor, f is the resonant frequency in hertz, L is the inductance in henrys, and R is the resistance in ohms. The effect the Q factor has on the sharpness of the resonant frequency and the bandwidth can be seen in figure 11. A higher Q factor results in a narrower bandwidth with the opposite true for a low quality factor.
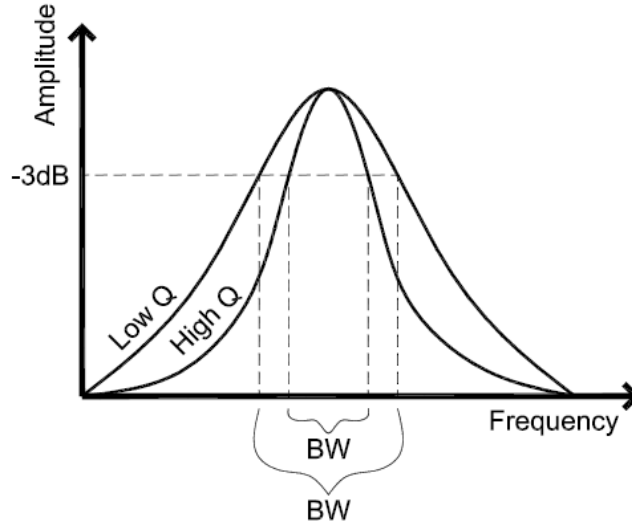
Figure 11. Relationship of Q value to BW.

The conductivity of the substrate also has an effect on the Q value. A semi-conductive substrate will tend to couple more energy to the substrate material as the frequency increases. This coupling to the substrate causes losses in the inductor [14]. The frequency where this begins to occur is dependent on the size of the spiral inductor.

4.2   Design Factors

The theoretical design of resonant sensors is an involved process. Several key parameters must be known to accurately make calculations and modeling. Characteristics of both the sensor and the substrate on which it is to be placed or embedded must be known. The sensor key parameters are inductance, capacitance, and resistance. In addition to the sensor's characteristics, the substrate's physical properties must be known to include not only the physical layup, but also permittivity and conductivity.

The sensor behaves differently when placed against the substrate due to the spiral-to-substrate interaction as opposed to free space. This interaction has an influence on the inductance, capacitance, and the resistance of the sensor. This in turn has an effect on the resonant frequency.

4.2.1   Inductance Value

The open circuit resonant sensor, as stated earlier, is a planar spiral and essentially an inductor. As with any inductor, the inductance value is composed of self and mutual inductance. The self-inductance is a measure of the magnetic field generated by a time-varying current. Mutual inductance is the measure of mutually coupled magnetic fields of adjacent traces with current flowing in the same direction. There are various empirical formulas that exist for calculating the inductance of a planar spiral [15]-[21]. These methods are mathematically intensive and were beyond the primary objective of a proof-of-concept design and, therefore, will not be presented. The Missouri Electromagnetic Compatibility Laboratory presented several simplified equations for various geometries. Equations (4) and (5) are for a circular spiral and a square spiral, respectively [22].

15

$$L_{circle} \approx N^2 R \mu_0 \mu_r \left[\ln\left(\frac{8R}{a}\right) - 2.0 \right]$$

<div align="right">Eq. (4)</div>

$$L_{square} \approx N^2 \frac{2\mu_0 \mu_r w}{\pi} \left[\ln\left(\frac{w}{a}\right) - 0.774 \right]$$

<div align="right">Eq. (5)</div>

Where (N) is the number of turns, (R) is the outer radius in centimeters, (a) is the wire radius in centimeters, (μ_0) is the permeability of free space, (μ_r) is the relative permeability of the medium (conductor), and (W) is the length of one side in centimeters. These are approximations and have a tolerance of 20% range as determined by comparison of calculated and measured data. These calculations are based upon the spiral in free space.

4.2.2   Capacitance Value

The capacitance is an inherent result of the width between the spiral traces and the interaction with the substrate which acts as a dielectric. The capacitance is considered to be parasitic and is minimal in a basic geometric spiral in free space or with a non-conductive substrate. As with the calculation of the inductance values, several equations exist for the calculation of the capacitance [15], [16], and [19]. To accurately calculate the capacitance of the sensor when placed upon a substrate the permittivity of the panel must be known.

The sensors for this project were tested in free space and on fiberglass composite panels. The fiberglass panels used were nonconductive and therefore the capacitance was considered to be minimal and more parasitic in both cases. The capacitance of the sensor was determined mathematically by manipulating the resonant frequency equation, equation (1).

4.2.3   Resistance Value

The total resistance of a planar spiral is a combination of series and parallel resistance. Series resistance is both dependent and independent on the frequency. The independent portion is essentially the direct current (D.C.) resistance of the wire, or in this case the trace, and is largely dependent on the total length. The frequency dependent portion of the overall resistance is due to the effects of eddy currents. The parallel resistance is a result of the finite resistance between the substrate material and the spiral conductor. Several equations exist to calculate the series and parallel resistance [16] and [19].

4.3   Design Geometry

The overall dimensions of the resonant sensor will play a significant role in inductance, capacitance, and resistance of the sensor. The size will factor into the trace width, spacing, and total length. The size of the composite material under test will also factor into the final design geometry. This project involved structural fiberglass test panels measuring 14 inches by 14 inches. This allowed for a multitude of possible sensor geometric layouts.

Sensors for this project were in the shape of polygonal spirals which included triangular, square, hexagonal, and circular. Spiral sensors of varying sizes for each shape were created. Figure 12 illustrates the four geometric shapes that were used.
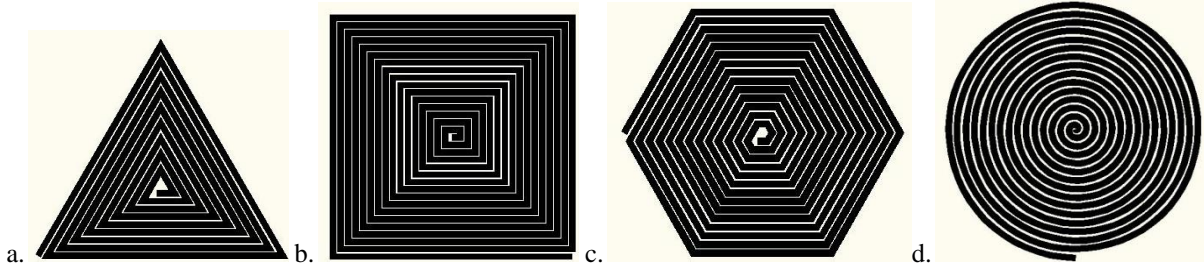
Figure 12. Spiral geometries utilized for the resonant sensors: (a) triangular, (b) square, (c) hexagonal, and (d) circular.

5.0   SENSOR DEVELOPMENT and FABRICATION

After gaining an understanding of the basic elements needed for the design, the development of the resonant sensor was undertaken. A process for the development and fabrication of the resonant sensors was created. The process outline was as follows:

- Theoretical Design

    - Desired resonant frequency

        - Geometry of sensor

        - Overall shape (circular, square, hexagon, octagon, triangle, etc.)

        - Trace width

        - Trace spacing

- Physical Design

    - Drawn using AutoCAD

- Fabricate

    - Klik-N-Kut used to cut copper sheet per design

5.1   Theoretical Design

The theoretical design process began with determining an initial resonant frequency for the sensor. It was determined that a variety of sensor shapes and sizes should be fabricated. This was decided upon in order to explore and characterize a wider range of sensors to gain further insight into the feasibility of the sensor for damage detection and diagnosis. In order to limit the number of variables, the outside dimension was the only change made to the sensors when designing sensors of varying size and shape. For simplicity, a determination was made to use a trace width and spacing that would result in a sensor's outer dimension incrementally equaling the whole inch.

17

The trace width and spacing was kept constant within all the designs. This allowed each subsequent larger sensor to increase the number of spiral turns. A trace width of 3/32 of an inch and a spacing of 1/32 of an inch was used.

5.2   Physical Design

The designs were done using Autodesk AutoCAD software. The use of computer-aided design (CAD) software allowed for an easy means to create sensor layouts of various dimensions and geometries, as well as rapid redesigns. Resonant sensors of the chosen geometries were designed with overall outer dimensions from two inches to fourteen inches in one inch increments. As stated in the previous section, the trace width and spacing between traces was kept constant for all designs. Figure 13 shows sensors ranging in size from two inches to nine inches and illustrates the constant stepped increase in the overall dimensions of the sensor.
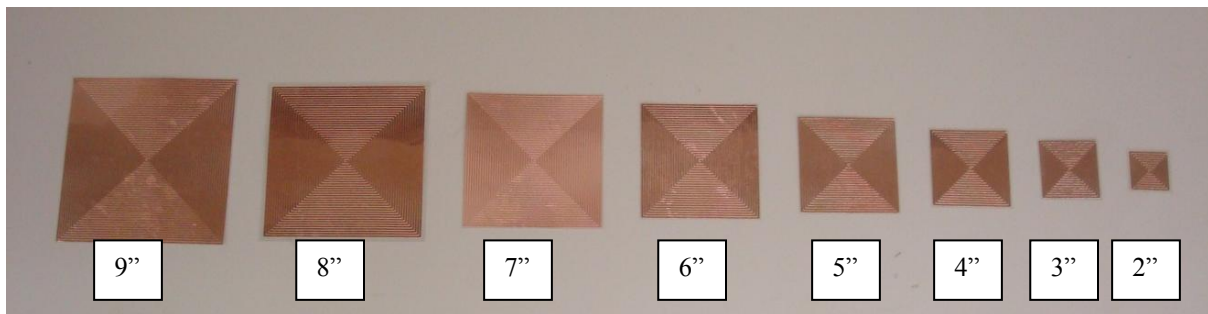
Figure 13. Square spirals ranging in outer dimensions from 2 inches to 9 inches.

5.3   Fabrication

The resonant sensors were fabricated from adhesive backed 1.25 mil thick copper sheets. The CAD designs were exported to a Klik-N-Kut (KNK) machine, figure 14, for cutting. The KNK machine provided a rapid means of cutting the copper sheet of the various geometries with a higher degree of accuracy and repeatability compared to using a straight edge and razor blade.

The first sensors were adhered directly to the fiberglass panel after cutting as seen in figure 17. This required a level of delicacy to prevent the sensor from becoming distorted in the transfer from the backing to the panel.

18
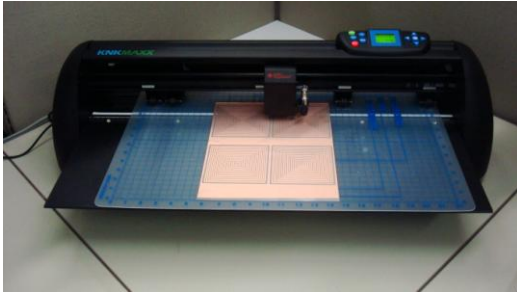
Figure 14. KNK Machine.
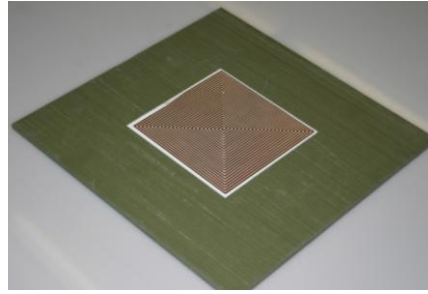
Figure 15. Sensor adhered directly to fiberglass panel.

Adherence of the sensor directly to the panel presented difficulties in testing additional sensors using the same panel. Removal of the sensor resulted in damage to the sensor rendering it unusable for repeated testing. This increased the time and cost between tests due to having to fabricate new sensors. A means to reduce the cost and time was devised. The sensors were laminated after cutting. This allowed for the sensors to be used repeatedly and enabled comparisons using the same sensor, not just the same design. The rigidity of the laminating plastic also made the sensors more robust which made handling simpler. The sensors could be easily reconfigured and the results allowed for a higher degree of repeatability. Laminating the sensors provided a cost savings in both time and materials. Figure 16 is an example of a hexagonal laminated sensor.
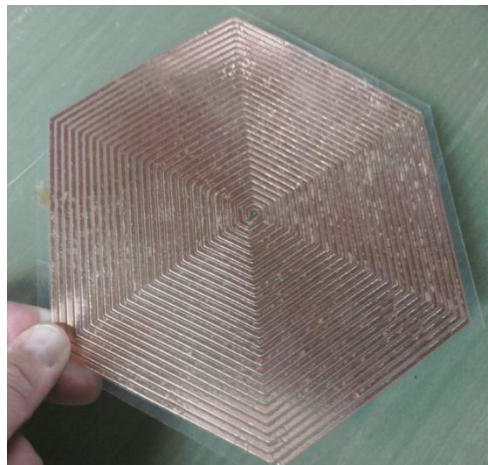
Figure 16. Laminated hexagonal spiral resonant sensor.

6.0   TEST PLAN

A test plan was developed to provide a methodical process to characterize the resonant sensor first in free space and then with it attached to the fiberglass composite panel. After characterizing the sensor and establishing a baseline measurement, the simulated damaged panels were utilized and the resulting measurements compared against the baseline. Conclusions could then be drawn. The test plan was broken down as follows:

- Normalize measurement system and determine background noise level for each transmit/receive antenna utilized

- For each sensor prototype:

    o Baseline measurements in free space

        ▪ Resonant frequency and harmonics

        ▪ Amplitude of resonant frequency and harmonics

        ▪ Waveform of resonant frequency and harmonics (Q, BW)

    o Baseline measurements with sensor attached to fiberglass panel

        ▪ Resonant frequency and harmonics

        ▪ Amplitude of resonant frequency and harmonics

        ▪ Waveform of resonant frequency and harmonics (Q, BW)

    o Measurements with sensor attached to damaged panels

        ▪ Resonant frequency and harmonics

        ▪ Amplitude of resonant frequency and harmonics

        ▪ Waveform of resonant frequency and harmonics (Q, BW)

- Comparison of measured data

- Conclusions

6.1 Normalization and Background Noise Level

Normalization of the measurement system was performed to eliminate the transmit/receive antenna characteristics from the sensor measurements for each antenna that was used and the background noise. This process involved taking a measurement using just the antenna and then subtracting this from future measurements. The background noise level measurement provides a baseline for comparison of the sensor's resonant frequency and harmonics amplitude to the background.

6.2 Sensor Free Space Characterization

Each sensor was characterized in free space. The characterization was used to establish a baseline in order to document the interaction of the substrate and the sensor. The baseline measurements included the resonant frequency, the harmonic frequencies within the span range, amplitude, and waveform (Q factor). This was done using various sized antennas. An example of the measured data can be found in Appendix A, Figures 18 and 20.

6.3 Sensor + Substrate Characterization

Once the initial baseline measurements were made the next step involved repeating the measurements with the various sensors attached to the composite fiberglass test panels. Each sensor was again characterized and a baseline was established that included the composite substrate. These baseline measurements included the resonant frequency, the harmonic frequencies within the span range, amplitude, and waveform (Q factor). This was also done using various sized antennas. An example of the measured data can be found in Appendix A, Figures 18,19, and 20.

6.4 Sensor Measurements of Damaged Panels

The data taken from the baseline measurements was analyzed and a determination was made as to which sensors would be used for testing of the damaged panels. The characteristics of the sensors selected for further testing were again measured utilizing the same methods as the baseline. An example of the measured data can be found in Appendix A, Figure 20.

6.5 Data Comparison

The collected data from the baseline free space, baseline undamaged composite panel, and damaged panel measurements was analyzed. Shifts in the resonant frequencies and harmonic frequencies were compared. Along with the frequency changes, the amplitudes and waveforms were compared for deviations. Examples of the measured data is presented in Appendix A.

7.0 TEST METHODS

The test plan was carried out based on experimental and computational methods. The experimental methods utilized a network analyzer and a magnetic response measurement system to test the functionality of the sensors. The computational method involved the use of computational software. As explained previously, the computational method was performed on a limited basis, as an aside, to provide a level of confidence for future use of the computational software.

7.1 Experimental Tools

7.1.1 Sensor Measurements with a Network Analyzer

Sensor characterizations and measurements were preliminarily explored with a network analyzer. The Agilent Performance Network Analyzer (PNA) system was used to search out the self resonance characteristics of several of the earlier developed sensors. The S-parameter model is obtained directly from measurements and will be useful for further design steps and analytical and computational model validation of planar geometric sensors.

The self resonance frequency of a sensor can be measured by using a network analyzer with a loop probe. The RF electromagnetic field is generated by connecting a loop probe to the output of the network analyzer set in reflection mode (S11 measurement). The equipment setup will directly display the system's resonant frequency. The network analyzer frequency sweep range was set up to be around the expected values of the sensors fundamental response and the first several harmonics. For the E8364C PNA, the lowest frequency available is 10 MHz, so this was used as the start frequency for the first

preliminary sensors tested. Ideally for the full range of sensors planned the start frequency would be lower. The stop frequency was set to 1000 MHz to establish a broad bandwidth over which to explore the fundamental resonance frequency of particular sensors and any associated higher order harmonics. The instrument was also configured to display data in the log magnitude format.

An initial background measurement was performed and the system normalized. The sensor under test was placed in the vicinity of the loop probe. The sensor and the loop probe were parallel and planar to one another. The probe was placed against the sensor. This orientation insures the maximum coupling of the electromagnetic field. The illuminating field was generated by the internal source of the network analyzer, transmitted through port one over a cable connected to the loop probe and then to the sensor. Upon excitation from the network analyzer the sensor under test resonates at a natural resonant frequency governed by the sensor's physical geometry. The sensor reflects, or more accurately re-radiates, a portion of the incident signal into the loop antenna connected to the network analyzer. This signal is received and processed by the network analyzer as an S_{11} measurement.

The resonant frequency corresponds to the minimum observed point on the S11 measurement logarithmic magnitude plot displayed on the network analyzer. Figure 17 shows the set-up using the PNA system. The sensor was first tested in free space away from the composite panel and then tested again with the sensor on the panel. Selected sensors were measured against the damaged panel.
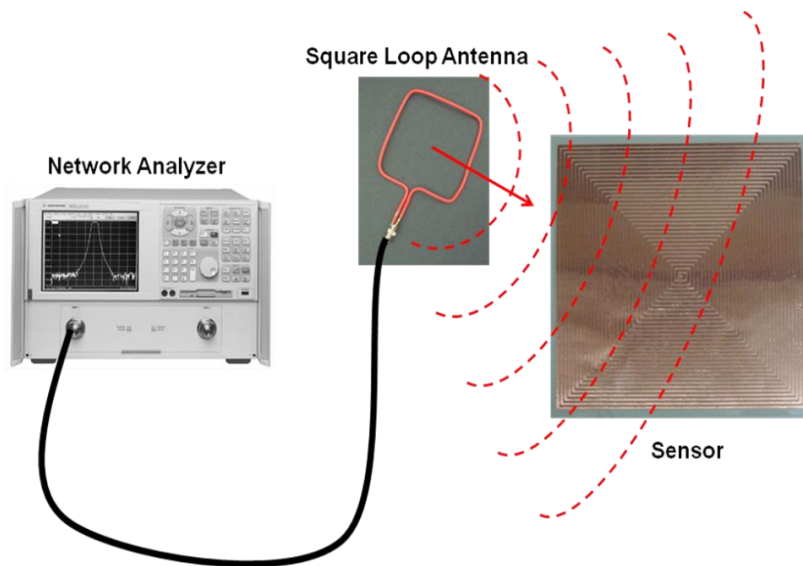
Figure 17. Measurement using Performance Network Analyzer (PNA) system.

7.1.2   *Sensor Measurements with a Magnetic Field Response Measurement System*

Dr. Stan Woodard and his group developed a Magnetic Field Response Measurement Acquisition System which was used as the primary data acquisition instrument for the characterizations of the developed resonant sensors. The components of the measurement system consisted of a loop antenna for transmitting and receiving magnetic fields, a processor for regulating the magnetic field transmission and reception, and software for control of the transmitted signal and for analyzing the responses received. A detailed description of the system can be found in NASA Technical Memorandum NASA/TM-2005-213518 "Magnetic Field Response Measurement Acquisition System" [23].

As with using the PNA, a background measurement was made. The sensor was first measured in free space and then again against the baseline panel. Select sensors were finally measured against the damaged panels.

7.2   Computational Tools

An attractive alternative for the trial and error measurement methodology is based on the use of electromagnetic simulation tools that allow predictive design. This is a process where the behavior of the electrical spirals can be predicted without the need for expensive and time consuming fabrication or measurements. Simulation tools allow a designer to characterize a virtual spiral, which is defined in a layout drawing environment. Most electromagnetic simulation tools produce frequency dependent S-parameters and are, therefore, virtual equivalents to the measurement-based technique. The choice of the simulation tool used is important.

Advantages of the simulation-based approach are that the designer has more flexibility to try variations of the spiral layouts or even optimize the spiral layouts so that a desired behavior is obtained. A typical simulation on a spiral, including the setup and interpretation of the results should not take more than half an hour. Alternative setups can be used to obtain better performing spirals, as a simulation on a new type of spiral is faster and cheaper than actual fabrication and testing. Simulation tools do require an accurate setup of the process parameters such as substrate and metallization characteristics. A process characterization step is therefore advised.

A characterization using simulation offers more flexibility during the design process of the spirals. The simulation provides predictive characteristics during the design process, and changes can be made easily to optimize and fine-tune the layout of the spiral for an optimal inductance value and quality factor. This optimization process can be automated. Parameter studies can reveal sensitivities and insight on how to improve the behavior of the spiral. A simulation-based approach requires an accurate, computationally efficient and user-friendly tool.

Computational analysis for this effort was done using FEKO. This method was used to validate a sensor's initial characteristics. The computational software was not utilized for simulating the sensor's response to a damaged panel because the altered material properties must be known.

8.0   CONCLUSIONS

A single resonant sensor of each geometric design was measured in free space and compared against each other in order to determine the most feasible design to further test and develop for this effort. It was determined that the square and hexagonal spirals provided the greatest amplitude above the noise floor as compared to the circular and triangular spirals.

The sensor acts as a rudimentary antenna, and it was determined that the resonant frequency increases as the size of the sensor decreases. This is important because the ability to penetrate the composite panel surface will most likely be dependent upon frequency.

A shift in the resonant frequencies and a decrease in the signal amplitudes occurred when the sensor was placed against the fiberglass composite panel. Also, it is important to notice that the greatest notable changes occurred to the higher resonant (harmonic) frequency when measuring the damaged panels.

The sensors show promise and ability to detect damage in fiberglass composite panels. The fiberglass panels are nonconductive and were a good starting point for the initial research into using the sensors for damage detection and diagnosis. Further testing will need to be accomplished to determine the ability of the sensor to function on carbon and other composite materials that have semi and conductive properties.

The ability to provide lightning protection and RF shielding needs to be explored. The variability of the sensor geometry and experimentation of the trace width and spacing will aide in further refinement. It may be possible to direct lightning currents based on the geometry of the sensor.

FEKO has demonstrated ability to accurately predict resonant frequencies and could possibly be used to design and verify future designs. This will greatly reduce the overall time required for design and testing. Further validation of the software's ability to be used in simulating shielding effectiveness needs to be performed by comparison of actual measured and simulated data.

Appendix A

Appendix A contains the measured data for the three inch through nine inch square spiral sensors and the four inch hexagonal spiral sensor. The two inch square sensor did not return a signal above the measured noise floor. This may be due in part to the receiving/transmitting antenna's size, initial radiating power output, or the scanned frequency range of the measurement system.

The test data is presented in graphical form. The sensor geometry, and transmitting/receiving loop antenna size, and measurement conditions (free space, attached to baseline fiberglass panel, or simulated damaged fiberglass panel) are indicated.
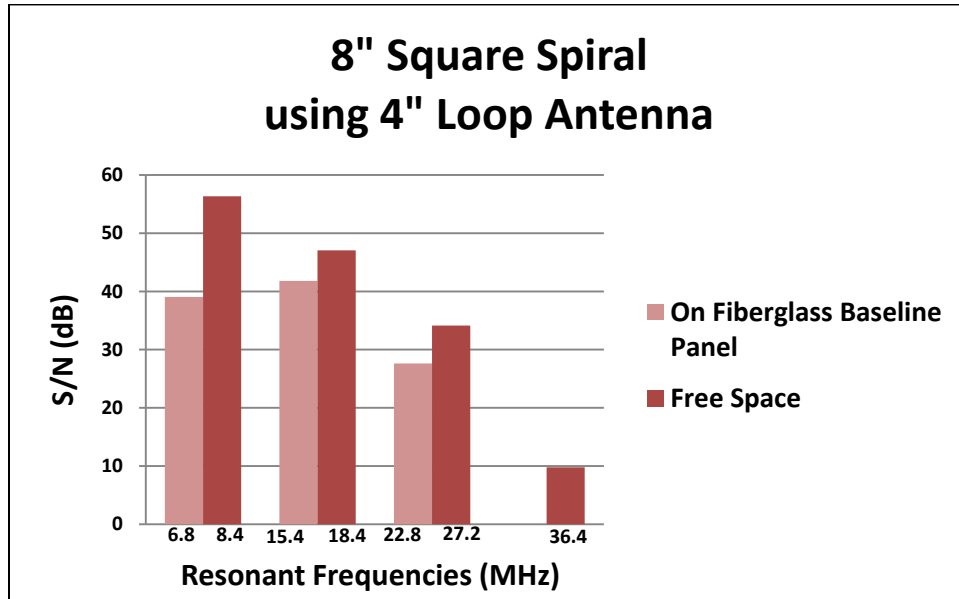
Figure 18. Comparison of the 8 inch square spiral sensor measured data in free space and against the fiberglass baseline panel.

Figure 18 is a comparison of the eight inch square spiral resonant sensor measured in free space and against the fiberglass composite panel. The graph shows that the resonant frequencies and the associated amplitudes decrease when placed against the fiberglass panel.
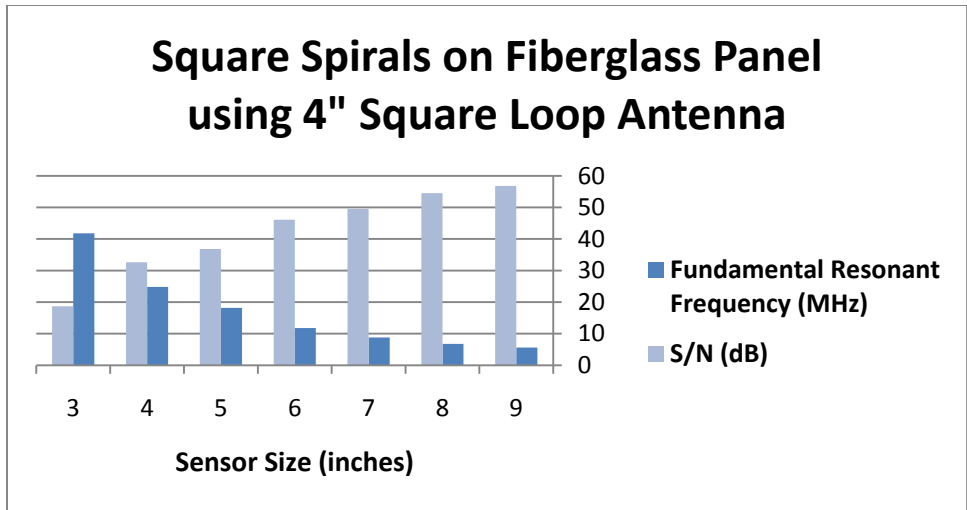
Figure 19. Comparison of Square spiral sensors sizes 3 inch through 9 inch against fiberglass panel using a four inch antenna.

Figure 19 is a comparison of the measured data of the square spiral sensors, ranging in size from three inches to nine inches. It can be seen that as the frequency decreases the amplitude increases.

The measurements of the four inch hexagonal spiral sensor using a four inch loop antenna are depicted in figure 20. The graph shows the resonant frequency and amplitude variations of the sensor measured in free space, against the baseline fiberglass panel, against the fiberglass panel with the simulated crack, and against the fiberglass panel with the simulated punctures. Most notably is the lack of change at the lower resonant and harmonic frequencies as compared to the second harmonic. The primary resonant and first harmonic frequencies show no change from the baseline panel. The third harmonic indicates both a frequency and amplitude deviation from the baseline, as well as the different types of damage. This is thought to be a result of the inability to penetrate the surface at higher frequencies and the simulated crack and punctures provided an "entry."
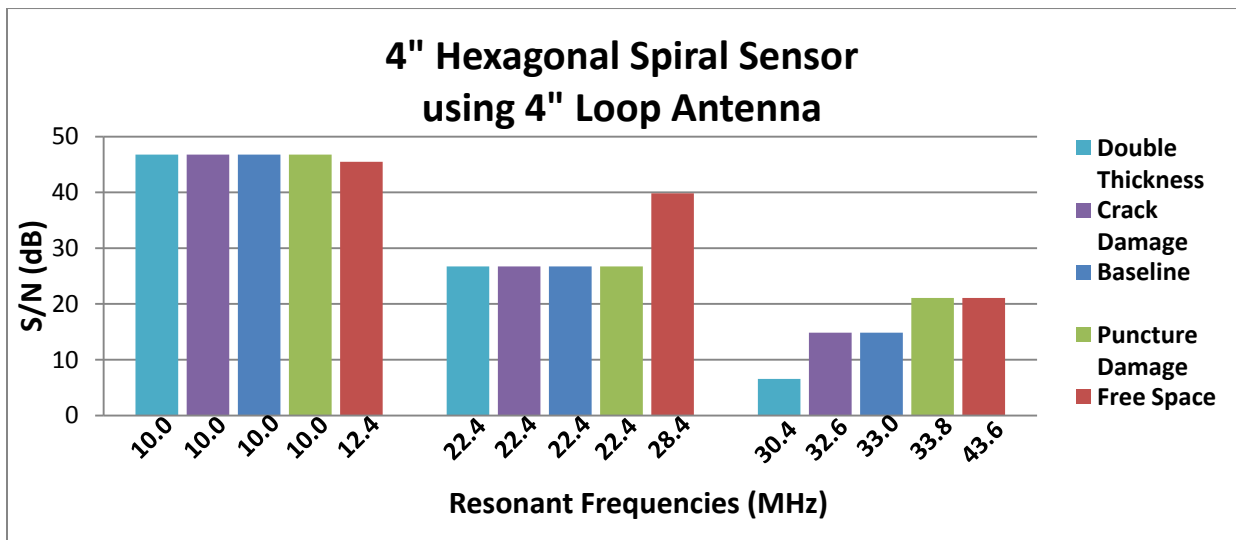
Figure 20. Comparison of the 4 inch hexagonal spiral sensor measurements.

REFERENCES

[1] Lamborghini unveils Sesto Elemento carbon fibre concept car. *REINFORCED plastics* 07 Oct. 2010: n. pag. Web. 10 Oct. 2010. http://www.reinforcedplastics.com/view/13027/lamborghini-unveils-sesto-elemento-carbon-fibre-concept-car/.

[2] "2011 Sea Ray 280 Sundancer | Sea Ray Boats and Yachts." *Sport Boats : Sport Cruisers : Sport Yachts : Yachts : Sea Ray Boats*. Web. 25 Aug. 2010. <http://www.searay.com/Page.aspx?pageId/10231/pmid/213256/280-Sundancer.aspx>.

[3] *Hexcel's Composite Materials for Wind Turbine Blades*. *Hexcel.com*. Hexcel. Web. 25 Aug. 2010. <http://www.hexcel.com/NR/rdonlyres/11D73FF4-D0A3-41B7-8B8D-B29BD0C87DE7/0/Hexcel_WindEnergy_Brochure2.pdf>.

[4] "Composite Horizons Inc : Military Aircraft." *Composite Horizons Inc : Home*. Web. 25 Aug. 2010. <http://www.chi-covina.com/pages/military-aircraft/>.

[5] "Composite Horizons Inc : Commercial Aircraft." *Composite Horizons Inc : Home*. Web. 25 Aug. 2010. <http://www.chi-covina.com/pages/commercial-aircraft/>.

[6] "Composite Horizons Inc : Satellite Components." *Composite Horizons Inc : Home*. Web. 25 Aug. 2010. <http://www.chi-covina.com/pages/satellite-components/>.

[7] Rusmee, Pichai. "High Strength Composites." *The University of Utah: Mechanical Engineering: Home*. Web. 11 Aug. 2010. <http://www.mech.utah.edu/~rusmeeha/labNotes/composites.html>.

[8] *Pilot's Handbook of Aeronautical Knowledge*. Oklahoma City, OK.: U.S. Dept. of Transportation, Federal Aviation Administration; Flight Standards Service, 2008. Print.

[9] "Helicopter Case Study - Why Study Materials Science?" *Why Study Materials Science? - What Is Materials Science?* Web. 18 Sept. 2010. <http://www.whystudymaterials.ac.uk/casestudies/helicopter.asp>.

[10] Workshops, -. "Composite Maintenance Workshop, July 2006, Chicago." *NIAR - National Institute for Aviation Research*. Web. 19 Aug. 2010. <https://www.niar.wichita.edu/niarworkshops/Workshops/ChicagoWorkshop2006/tabid/99/Default.aspx>.

[11] "Defects in Polymer Composites." *Polymer Engineering, Materials Testing, Inspection, Research, Development, Resistance, UK*. Web. 25 Aug. 2010. <http://www.merl-ltd.co.uk/2003_materials/composites06.shtml>.

[12] Chuantong Wang; Woodard, S.E.; Taylor, B.D.; , "Sensing of multiple unrelated tire parameters using electrically open circuit sensors having no electrical connections," *Sensors Applications Symposium, 2009. SAS 2009. IEEE* , vol., no., pp.142-147, 17-19 Feb. 2009. Web. 19 Aug. 2010. < http://ieeexplore.ieee.org/stamp/stamp.jsp?tp=&arnumber=4801795&isnumber=4801760>

[13] Shrader, Robert L. *Electronic Communication*. Fifth ed. New York: McGraw-Hill, 1985.

[14] Shukla, Neeraj KR., Shilpi Birla, and R.K.Singh, "New Modeling Technology for Spiral Inductors for Ultra Wideband Applications", IACSIT International Journal of Engineering and Technology Vol. 2, No.1, ISSN: 1793-8236, February, 2010.

[15] Chen, Wai-Kai. "RF Passive IC Components." *The VLSI Handbook*. Boca Raton, FL: CRC, 2000.

[16] Yue, Patrick C., and Simon S. Wong. "Physical Modeling of Spiral Inductors on Silicon." *IEEE Transactions on Electron Devices* 47.3 (2000): 560-68. *IEEE Xplore*. Web. 12 Aug. 2010. <http://ieeexplore.ieee.org/stamp/stamp.jsp?tp=&arnumber=824729>.

[17] Greenhouse, H. M. "Design of Planar Rectangular Microelectronic Inductors." *IEEE Transactions on Parts, Hybrids, and Packaging* PHP-10.2 (1974): 101-09. Web. 12 Aug. 2010. <http://ieeexplore.ieee.org/stamp/stamp.jsp?tp=&arnumber=1134841>.

[18] Mohan, Sunderarajan S., Maria Del Mar Hershenson, Stephen P. Boyd, and Thomas H. Lee. "Simple Accurate Expressions for Planar Spiral Inductances." *IEEE Journal Of Solid-State Circuits* 34.10 (1999): 1420-421. Web. 10 Sept. 2010. <http://www.stanford.edu/~boyd/papers/pdf/inductance_expressions.pdf>.

[19] C.R. Neagu, H.V. Jansen, A. Smith, J.G.E. Gardeniers, M.C. Elwenspoek, "Characterization of a planar microcoil for implantable microsystems, Sensors and Actuators" Volume 62, Issues 1-3, Proceedings of Eurosensors X, July 1997, Pages 599-611. <http://www.sciencedirect.com/science/article/B6THG-3T4D01G-W/2/ac06559ccdaaa9bb76c63cac7611ea92>

[20] Balakrishnan, A.; Palmer, W.D.; Joines, W.T.; Wilson, T.G.; , "Inductance of planar rectangular-spiral strip conductors for low-profile inductors," *Power Electronics Specialists Conference, 1992. PESC '92 Record., 23rd Annual IEEE* , vol., no., pp.1401-1408 vol.2, 29 Jun-3 Jul 1992 < http://ieeexplore.ieee.org/stamp/stamp.jsp?tp=&arnumber=254749&isnumber=6473>

[21] Lee, Youbok. "AN710 - Antenna Circuit Design - Application Notes - Details." *Microchip Technology Inc.* 2003. Web. 14 Aug. 2010. <http://www.microchip.com/stellent/idcplg?IdcService=SS_GET_PAGE&nodeId=1824&appnote=en011776>.

[22] "Missouri S&T." *Missouri S&T, Electromagnetic Compatibility Laboratory*. Web. 11 Aug. 2010. <http://emclab.mst.edu/inductance/index.html>.

[23] Stanley E. Woodard, Qamar A. Shams, Bryant D. Taylor and Robert L. Fox, "Magnetic Field Response Measurement Acquisition System," NASA/TM-2005-213518 Langley Research Center, Hampton, Virginia, February, 2005.

REPORT DOCUMENTATION PAGE		*Form Approved* *OMB No. 0704-0188*

The public reporting burden for this collection of information is estimated to average 1 hour per response, including the time for reviewing instructions, searching existing data sources, gathering and maintaining the data needed, and completing and reviewing the collection of information. Send comments regarding this burden estimate or any other aspect of this collection of information, including suggestions for reducing this burden, to Department of Defense, Washington Headquarters Services, Directorate for Information Operations and Reports (0704-0188), 1215 Jefferson Davis Highway, Suite 1204, Arlington, VA 22202-4302. Respondents should be aware that notwithstanding any other provision of law, no person shall be subject to any penalty for failing to comply with a collection of information if it does not display a currently valid OMB control number.
PLEASE DO NOT RETURN YOUR FORM TO THE ABOVE ADDRESS.

1. REPORT DATE *(DD-MM-YYYY)* 01-01-2011	2. REPORT TYPE Contractor Report	3. DATES COVERED *(From - To)*

4. TITLE AND SUBTITLE	5a. CONTRACT NUMBER
Open Circuit Resonant Sensors for Composite Damage Detection and Diagnosis	NNL10AM25T
	5b. GRANT NUMBER
	5c. PROGRAM ELEMENT NUMBER

6. AUTHOR(S)	5d. PROJECT NUMBER
Mielnik, John J.	
	5e. TASK NUMBER
	5f. WORK UNIT NUMBER 648987.02.04.07.20

7. PERFORMING ORGANIZATION NAME(S) AND ADDRESS(ES) NASA Langley Research Center Hampton, VA 23681-2199	8. PERFORMING ORGANIZATION REPORT NUMBER

9. SPONSORING/MONITORING AGENCY NAME(S) AND ADDRESS(ES) National Aeronautics and Space Administration Washington, DC 20546-0001	10. SPONSOR/MONITOR'S ACRONYM(S) NASA
	11. SPONSOR/MONITOR'S REPORT NUMBER(S) NASA/CR-2011-216884

12. DISTRIBUTION/AVAILABILITY STATEMENT
Unclassified - Unlimited
Subject Category 33
Availability: NASA CASI (443) 757-5802

13. SUPPLEMENTARY NOTES
Langley Technical Monitor: Sandra V. Koppen

14. ABSTRACT
Under the Integrated Vehicle Health Management (IVHM) program work was begun to investigate the feasibility of sensor systems for detecting and diagnosing damage to aircraft composite structures and materials. Specific interest for this study was in damage initiated by environmental storm hazards and the direct effect of lightning strikes on the material structures of a composite aircraft in flight. A series of open circuit resonant sensors was designed, fabricated, characterized, and determined to be a potentially viable means for damage detection and diagnosis of composite materials. The results of this research and development effort are documented in this report.

15. SUBJECT TERMS
Open circuit; Resonant; Sensors; Composite materials; Composite structures; Damage detection

16. SECURITY CLASSIFICATION OF:			17. LIMITATION OF ABSTRACT	18. NUMBER OF PAGES	19a. NAME OF RESPONSIBLE PERSON STI Help Desk (email: help@sti.nasa.gov)
a. REPORT	b. ABSTRACT	c. THIS PAGE			19b. TELEPHONE NUMBER *(Include area code)*
U	U	U	UU	33	(443) 757-5802

Standard Form 298 (Rev. 8-98)
Prescribed by ANSI Std. Z39.18